Kazemeini, S. H., Juhlin, C., Zinck-Jorgensen, K., Norden, B. (2008): Application of the continuous wavelet transform on seismic data for mapping of channel deposits and gas detection at the CO2SINK site, Ketzin, Germany. - Geophysical Prospecting, 57, 1, 111-123

DOI: 10.1111/j.1365-2478.2008.00723.x.

Abstract

Conventional seismic data are band limited and, therefore, provide limited geological information. Every method that can push the limits is desirable for seismic data analysis. Recently, time-frequency decomposition methods are being used to quickly extract geological information from seismic data and, especially, for revealing frequency dependent amplitude anomalies. Higher frequency resolution at lower frequencies and higher temporal resolution at higher frequencies are the objectives for different time-frequency decomposition methods. Continuous Wavelet Transform techniques, which are the same as narrow-band spectral analysis methods, provide frequency spectra with high temporal resolution without the windowing process associated with other techniques. Therefore, this technique can be used for analyzing geological information associated with low and high frequencies that normally cannot be observed in conventional seismic data. In particular, the Continuous Wavelet Transform is being used to detect thin sand bodies and also as a direct hydrocarbon indicator. This paper presents an application of the Continuous Wavelet Transform method for mapping of potential channel deposits, as well as remnant natural gas detection by mapping low frequency anomalies associated with the gas. The study was carried out at the experimental CO_2 storage site at Ketzin, Germany (CO_2SINK). Given that reservoir heterogeneity and faulting will have significant impact on the movement and storage of the injected CO_2 our results are encouraging for monitoring the migration of CO_2 at the site. Our study confirms the efficiency of the Continuous Wavelet Transform decomposition method for detection of frequency dependent anomalies which may be due to gas migration during and after the injection phase and in this way it can be used for real-time monitoring of the injected CO_2 from both surface and borehole seismics.

Introduction

CO_2SINK, an European integrated research project that was initiated in April 2004, is geared towards studying several aspects of geological storage of CO_2 in saline aquifers at onshore sites as a means of reducing greenhouse gas emissions (Förster et al. 2006). Main objectives of the project are to (1) advance the understanding of the science and practical processes involved in underground storage of CO_2 to reduce emissions of greenhouse gases to the atmosphere, (2) build confidence towards future European CO_2 geological storage, and (3) provide operational field experience to aid in development of harmonized regulatory frameworks and standards for CO_2 geological storage. Particular attention is being given to the monitoring component of geological storage. That is, can migration of CO_2 within the reservoir, through artificial pathways (boreholes) and leakage via faults be mapped? Also, how will the quality of geological seals, as well as the reservoir itself, change with time as CO_2 is injected and dissolves in brine-filled pores and/or reacts with reservoir minerals.

The selected CO_2SINK injection site, the Ketzin anticline, is located about 25 kilometer west of Berlin, Germany (Figure 1). Town and natural gas had earlier been stored at the site from the 1970s until 2000 at depths of 250 m to 400 m in Jurassic sandy layers sealed with a thick layer of Rupelian clay and interbedded mudstone. However, the target reservoir in the CO_2SINK project is a deeper saline aquifer within the upper Triassic Stuttgart Formation at depth of 625 m to 700 m at the injection site. Several factors played a role in choosing the Ketzin site. These included (1) a favorable geological setting for CO_2 storage, (2) the close proximity to a large metropolitan area for evaluating the public acceptance of a CO_2 storage site, (3) the presence of the natural gas storage infrastructure and (4) the possession of the mining rights of the site by one of the project partners.

An important component within the CO_2SINK project monitoring activities is seismic monitoring. Methods that will be applied include cross-well, vertical seismic profile (VSP), moving source

profiling (MSP), 2D and 3D time lapse techniques. Initially, a pilot seismic study was carried out in 2004 to determine optimum acquisition parameters and to test the seismic response of the Ketzin site (Yordkayun et al. 2007). The pilot survey was followed by a 3D baseline seismic survey with 12 km^2 of sub-surface coverage in 2005 (Juhlin et al. 2007). The 3D survey showed clear E-W trending faults on the crest of the Ketzin anticline, a clear signature from remnant gas in the sandy Jurassic formations, and a gas chimney associated with an E-W trending fault. In addition, there were indications that the sandy reservoir channels within the heterogeneous Stuttgart Formation could be mapped.

In this paper we investigate how the Continuous Wavelet Transform can be applied to the migrated 3D data in order to supply further information on the structure and physical properties of the rocks within the Ketzin anticline. Mapping the internal structure of the Stuttgart Formation is especially challenging since it is lithologically heterogeneous, consisting of sandy channels (reservoir pathways) within floodplain or playa-type facies sediments. The dimensions of these sand bodies remain a matter of debate (Frykman et al. 2006) and they cannot easily be mapped by conventional seismic methods. It is possible that sandy channels can be better mapped by applying the Continuous Wavelet Transform and decomposing the data into different frequency components. Knowing the geometry of sandy channels in the vicinity of the injection site will have importance for evaluating future seismic time lapse studies and hydrological modeling. Another application of the Continuous Wavelet Transform in this study is mapping the spatial extent of the remnant gas in the Jurassic sandstones and, thereby, investigating the sealing properties of the faults that cut these rocks. Stored natural gas has migrated from at least one of the faults to upper levels as evidenced by a gas chimney in the western part of the crest of the Ketzin structure. However, the gas has not reached the surface and is held back by another natural barrier, obviously not affected by the fault system. The Continuous Wavelet Transform analysis allows for fast inspection of the data for locating the gas chimney and adds an important complement to the conventional interpretation.

Geological Setting

The Ketzin anticlinal structure is located in the Northeast German Basin, a sub-basin in the eastern part of the Southern Permian Basin, and is bounded by the Elbe Fault system in the south, the Trans-European Suture Zone and the North Danish Basin in the north, the Northwest German Basin in the west and the Polish Trough in the east. The structural and depositional setting of the basin are characterized by polyphase uplifting and subsidence events (Ziegler, 1990; Scheck and Bayer 1999). Although somewhat poorly constrained in time, development of the basin began by initial rifting in the early Permian and was followed by subsidence and the deposition of Permian clastic sediments and the Upper Permian Zechstein salt. Since the early Triassic, several deformation phases have modified the Upper Permian Zechestein salt, resulting in the development of pillows, walls, and diapirs that also deformed the Mesozoic overburden into a system of anticlines and synclines. The Ketzin structure, in the eastern part of the Roskow-Ketzin double anticline, formed above an elongated salt pillow situated at a depth of 1500-2000 m. The axis of the anticline strikes NNE-SSW and its flanks dip gently at about 15° (Förster et al. 2006). Directly above the salt, structurally deformed Triassic and Lower Jurassic formations are present. Stratigraphic successions indicate a first gentle uplift of the Ketzin anticline in the early Triassic followed by two major phases of uplift, one at 140 Ma and a second at 106 Ma. The first major uplift resulted in erosion of the uppermost Lower Jurassic, the Middle and the Upper Jurassic formations. A second uplift resulted in the erosion of Lower Cretaceous rocks. There was no deposition during Upper Cretaceous time, since the area was part of a structural high then (Förster et al. 2006). Oligocene transgressive sediments, resting above the Jurassic sediments, unaffected by anticlinal uplift, are the first indication of regional downwarping of the central parts of the Northeast German Basin, which is continuing to the present day (Förster et al. 2006).

The target reservoir at the Ketzin site, the lithologically heterogeneous Upper Triassic Stuttgart

Formation, is about 75 m thick at depths of 500 m to 700 m. It contains sandy channel-facies rocks of good reservoir properties, and also muddy flood-plain-facies rocks of poor reservoir quality (Förster et al. 2006). The sedimentary setting of the target reservoir is a system of incised-valley deposits, where sandy channel belts have formed by amalgamation of individual fluvial channels. The channels are incised into flood-plain-facies or playa-type facies sediments, possibly including some levee deposits and overbank crevasse splays. Considering the sedimentary setting of the Stuttgart Formation, the thickness of the sandstone intervals may vary from 1 m up to 30 m where sub-channels are stacked. The width of the channel-string system is between several tens of meters to several hundreds of meters (Wurster, 1964).

Above the Stuttgart Formation lie the Weser and Arnstadt Formations, consisting of a mudstone and a 10-20 m thick anhydrite layer (the seismic K2 reflector at the top of the Weser Formation) (Figure 2). These rocks form an approximately 200 m thick caprock above the reservoir. Further up, at 250 m to 400 m depth, additional aquifer-aquitard systems are present in the form of Jurassic sandstone interbedded with mudstone, claystone and siltstone that form a multi-aquifer system. This system is covered by an 80-90 m thick Tertiary clay (Rupelton) that acts as a caprock for these Jurassic sandstones. This clay separates the saline waters in the deeper aquifers from the non-saline groundwater in shallow Quaternary aquifers. At some locations, local erosion of the Rupelton aquitard results in ascending saline waters that mix with the fresh waters of the shallow aquifers (Förster et al. 2006).

Low frequency shadow zones

Taner et al. (1979) were one of the first investigators to observe anomalously low frequency components in the seismic signal associated with hydrocarbon reservoirs. However, they were not able to provide a clear mechanism to explain the phenomena. Recent developments of spectral

decomposition methods allow frequency dependent amplitude anomalies to be rapidly mapped, resulting in better reservoir delineation and characterization (e.g. Castagna et al. 2003; Sinha et al. 2005; Goloshubin et al. 2006 and Wang 2007). In many of these mapping studies the "Low-frequency gas shadow" is observed. Castagna et al. (2003) hypothesized that the involved mechanisms are more complicated than only conventional attenuation of the higher frequencies, especially for thin reservoir layers where the travel path is not sufficient for any significant absorption. That it is not a question of attenuation is supported in a recent study (Wang 2007) where the low frequency shadow beneath a carbonate gas reservoir is still observed after inverse Q filtering. Eborm (2004) described 10 mechanisms categorized into stack (processing artefacts) related and non-stack related (physics) processes. Recently, Goloshubin and Korneev (2000) carried out several studies in an attempt to explain frequency dependent reflectivity based on a non-elastic reservoir model where Biot theory is not valid (Goloshubin and Bakulin 1998; Goloshubin and Korneev 2000; Korneev et al. 2004). Although a number of researchers since the Taner et al. (1979) paper have observed and studied the possible mechanisms behind the low-frequency shadow phenomena in association with hydrocarbon reservoirs no adequate explanation for its existence has been accepted. Processing artefacts can still not be ruled out (Castagna et al. 2003).

The Ketzin 3D seismic data set

Data were acquired using overlapping templates with 5 receiver lines containing 48 active channels in each template. Nominally, 200 source points were activated in each template using an accelerated weight drop source giving a nominal fold of 25, although the number of actual source points in each template varied due to logistics. In order to be time efficient and minimize potential of producing artefacts, the processing flow was kept relatively simple. Table 1 shows the main processing steps applied to the 3D data set. The Continues Wavelet Transform study in this paper has been carried out on the migrated 3D seismic data. Data quality is generally good with the uppermost 1000 m being well

imaged (Juhlin et al. 2007). Particularly clearly imaged is the K2 horizon (the top Weser Formation) over the entire area. The base of the target Stuttgart Formation lies about 80 ms below the K2 marker horizon. By summed amplitude mapping of the Stuttgart Formation a structure is outlined that could represent a sandy channel within the formation near the injection site (Juhlin et al. 2007). Vintage 2D seismic data from the 1960s show an anticlinal structure for the Ketzin area which was confirmed by the new 3D survey (Juhlin et al. 2007). The 3D data show an E-W striking central graben on the top of the Ketzin anticline that extends down to the target horizon and with about 30 m of throw on the faults. No faults are imaged near the Ketzin injection site. Remnant gas, cushion and residual gas, is present near the top of the anticline in the depth interval of about 250 m to 400 m and has a clear seismic signature on the 3D seismic data, both higher amplitudes in the reservoir horizons and velocity pulldown are observed. Amplitude mapping of these remnant gas horizons shows that they do not extend as far south as the injection site, which is located on the southern flank of the anticline (Figure 3). However, the injected CO_2 is expected to migrate within the reservoir formation up towards the top of the anticline, implying that changes in the remnant gas concentration may have to be taken into account when monitoring the injected CO_2. An amplitude anomaly, a gas chimney, along the E-W striking fault system near the top of the anticline shows that stored or remnant gas either has been or is presently migrating out of the upper reservoir formation.

Calibration of the seismic data

At the time of conventional interpretation of the 3D seismic data reported on in Juhlin et al. (2007) the only well to target depth in the area was the Ktzi 163/69 borehole, which is located outside of the 3D survey area (Figure 3). An initial attempt to tie this well to the 3D seismic data using data acquired along a 2D pilot line (Yordkayhun et al. 2007), passing over the well and into 3D survey area, failed due to lack of sonic and density logs extending from the surface to total depth. In this study we use the

gamma log from this well to generate a synthetic sonic log form surface to a depth of 680 m, an interval where no sonic log data exist, in order to overcome the missing data problem. We can do this since the sonic and gamma logs show a clear linear relationship to one another over those intervals where the sonic has been recorded. The synthetic seismogram generated from this partly synthetic sonic log matches well with the 2D section recorded in the vicinity of the well (Figure 4a). Is is now fairly clear which reflections correspond to the near top and base of the Stuttgart Formation at this location. For further calibration, we use the sonic log from the newly drilled (summer of 2007) expected injection well, CO2 Ktzi 200/2007 well, to generate and an additional synthetic seismogram and tie this seismogram directly to the 3D seismic survey (Figure 4b). At the location of CO2 Ktzi 200/2007 there is no clear seismic event corresponding to the near top of the Stuttgart Formation, however, the base of the formation corresponds to a relatively clear event.

Continuous Wavelet Transform decomposition methodology

In recent years, spectral decomposition has been frequently used to map temporal bed thickness (Partyka et al. 1999) and for direct hydrocarbon detection (Castagna et al. 2003). Various techniques have been developed for the spectral decomposition of seismic data. The aim of all these techniques is to decompose a seismic signal into its constitute components in order to obtain more geological information. For example, the discrete Fourier transform (DFT) is a traditional frequency decomposition method. The transform determines the relative strength of each frequency component of the entire signal, but does not provide information on how the frequency content changes with time. Therefore, the discrete Fourier transform method is not suitable for analysis of non-stationary signals since it is unable to localize frequency variations over time.To handle this problem, the short time Fourier transform (STFT) method is widely used for decomposition of non-stationary signals. The basic idea in the short time Fourier transform is to divide up a non-stationary signal into small segments of assumed stationary portions and calculate the Fourier transform for each segment. In

performing this segmentation a “window function” is chosen and multiplied with the signal. One problem with this approach is that the fixed width “window function” results in limited resolution. A short time window provides appropriate time resolution, but poor frequency resolution. If a wider time window is chosen, frequency localization is improved, but time resolution is decreased. The Continuous Wavelet Transform decomposition can be used as an alternative approach to the short time Fourier transform decomposition to overcome this resolution problem. In the Continuous Wavelet Transform, as in the short time Fourier transform, the signal is multiplied with a function similar to a “window function”, but the width of the window is not fixed. The time window width is allowed to vary depending upon the frequency that is being considered. This variation in width results in a windowing function that is known as a “wavelet function” .

Mathematically, the Continuous Wavelet Transform is defined as the sum over all time of the signal $f(t)$ multiplied by scaled and shifted versions of the analyzing wavelet function ψ :

$$C(scale, translation) = \int_{-\infty}^{+\infty} f(t)\psi(scale, translation, t)dt$$

$$C(\sigma, \tau) = \int_{-\infty}^{+\infty} \frac{1}{\sqrt{\sigma}} \overline{\psi}\left(\frac{t-\tau}{\sigma}\right) f(t)dt$$

where the term $\frac{1}{\sqrt{\sigma}} \overline{\psi}\left(\frac{t-\tau}{\sigma}\right)$ is a family of scaled and shifted wavelets and σ and τ are scale and shift parameters, respectively (Sinha et al. 2005). The output of the Continuous Wavelet Transform is a series of wavelet coefficients, *C*, which are a function of these scale and shift parameters. Multiplying each coefficient by the appropriately scaled and shifted wavelet yields the constituent wavelets of the original signal. The fact that the Continuous Wavelet Transform decomposes an input signal into its constituent wavelets allows, via the superposition principle, the frequency spectrum of the input signal to be calculated by summing the frequency spectra of the wavelets. Therefore, the resulting time-scale map (scalogram) can be converted to a time-frequency spectrum by associating a pseudo-frequency to

the scale. One way to do this is to compute the center frequency (f_c) of the wavelet and to use the relationship $f_\sigma = f_c/\sigma\Delta$ where f_σ is the pseudo-frequency corresponding to scale σ and Δ is the sampling period.

An important step in Continuous Wavelet Transform decomposition is selecting the "wavelet function", also known as the "mother wavelet". Although there is no optimum wavelet among the different commonly used wavelets, some consideration should be given to selecting the appropriate mother wavelet. For example, the side lobes of the Morlet wavelet reduce the vertical resolution of the Continuous Wavelet Transform (Castagna and Sun 2006). However, the wavelet is sensitive to energy absorption and phase distortion and is, therefore, a suitable choice for studies of the acoustic properties of gas reservoirs that are thick enough to be resolved on seismic data (Wang 2007). Once the mother wavelet is selected, a series of scaled and shifted wavelets are produced. In contrast to the short time Fourier transform method, which has a fixed limited resolution, the Continuous Wavelet Transform gives good time resolution at higher frequencies and good frequency resolution at lower frequencies. In this paper, we used the Mexican Hat wavelets for localizing the channel and Morlet wavelets for investigating the spatial extent of the remnant gas..

Application of the Continuous Wavelet Transform **decomposition method to field data**

We focus our attention on two zones from the 3D survey. The first one extends from the top to the base of the Stuttgart Formation for channel mapping within the CO_2 injection target horizon and the second one is from 215 ms to 300 ms, the approximate time window where remnant gas is present. Figure 5 shows power spectra for the later zone of interest.

For channel mapping within the Stuttgart Formation, which is 50-60 ms thick at the Ketzin structure, we compare results from the Continuous Wavelet Transform analysis with an amplitude horizon map located 45 ms above the picked base of the Stuttgart Formation. On the amplitude map (Figure 6a) a

possible curved channel feature (Juhlin et al. 2007) is weakly indicated at the top and middle left of the investigated area. The 25 Hz Continuous Wavelet Transform frequency map for the same horizon (Figure 6b) shows a similar feature, but the channel appears much clearer since other frequency components are not interfering with the signal. Superposition of the separate frequency components destroys the pattern of the geological features in the amplitude map. The 35 Hz horizon slice (Figure 6c) shows that possible thinner channel sediments continue south of the injection well location. The channel in this area is not thick enough to appear on the 25 Hz frequency and amplitude maps. Therefore, the channels disappear and reappear again. The 45 Hz map shows more detail of the possible channel system south of the injection well location (CO2 Ktzi 200/2007). The high energy feature on the right hand side of the 25, 35 and 45 Hz frequency maps can be interpreted as sand bodies deposited in an additional channel. Meandering, avulsion and crevasses are common in fluvial sedimentary environments and we may be seeing some of these feature at the Ketzin site.

We have also applied the Continuous Wavelet Transform technique to detect and map remnant gas in the shallower parts of the Ketzin structure. Natural gas had been injected and stored in the Upper Jurassic formations in the Ketzin structure from the 1970s until 2000. Since the gas was injected into several layers and later migrated upwards, the picking of a distinct seismic event at the top of the gas storage reservoir is difficult. Figure 7 shows amplitude brightening on the seismic data due to remnant gas accumulation. Several gas/water contact flat spots indicate several reservoir layers interbedded with shale layers. For quick mapping of the remnant gas, we performed Continuous Wavelet Transform analysis on a slice at 215 ms, some 10 ms below the top gas layer and at 300 ms, almost 25 ms below the deepest gas layer. This deeper slice from below the deepest gas/water contact was chosen in order to detect possible low frequency shadows beneath the gas accumulation zone.

Figure 8 shows 20, 40 and 60 Hz common frequency slices at 215 ms (8a, 8b and 8c) and 300 ms (8d,

8e and 8f). The maximum gas distribution area based on a report by the "Untergrundspeicher- und Geotechnologie-Systeme GmbH" (UGS) (the operator of the natural gas storage facility at Ketzin) is shown as a dotted line. At 20 Hz, the near top gas slice (Figure 8a) is not very bright. Some higher amplitudes near the main faults can be interpreted as low frequency shadows below the gas that has migrated to shallower levels. The 20 Hz slice at 300 ms (Figure 8d) shows a strong signal below the gas accumulation zone and is interpreted as a low frequency shadow associated with the gas above it. By comparing Figure 8b with Figure 8d it can be seen that the shadow has shifted outwards from the anticline top in comparison to the main gas accumulation. At higher frequencies (40 and 60 Hz) the near top gas slices (Figures 8b and 8c) show clear bright spots which clearly match the "Untergrundspeicher- und Geotechnologie-Systeme GmbH" (UGS) reported gas distribution area. In the 40 and 60 Hz frequency slices, below the gas accumulation zone (Figures 8e and 8f), the strong shadow seen in Figure 8b and 8c has disappeared. The similarity slice at 215 ms (Figure 9) indicates that the distribution pattern of gas and particularly the migration pattern (results from Figures 8a and 8b) are in good accordance with the fault pattern.

Discussion and Conclusion

We have successfully used the Continuous Wavelet Transform decomposition method to map thin beds in seismic data. Results from this study are important for the reservoir modelling and site characterization phases of the CO_2SINK project at Ketzin. Our Continuous Wavelet Transform analysis suggests the presence of meandering channel beds within the Stuttgart Formation, a highly plausible geological situation. The seismic monitoring phase of the project may allow our Continuous Wavelet Transform interpretation to be verified.

We have also shown that the Continuous Wavelet Transform method can detect and map remnant injected gas. The information obtained from decomposed common frequency slices cannot be obtained from conventional seismic amplitude slices. For instance, based on this study we conclude that there is

no gas at 300 ms where the amplitude is still bright on the crest of the Ketzin anticline in comparison with the flank. The higher amplitudes are due to the gas accumulation zone causing a low frequency shadow.

As in the case discussed by Wang (2007), our study also shows the low frequency component below gas bearing rocks are higher than above. Furthermore, the low frequencies are not observed from deeper horizons, supporting the idea that it cannot be simple attenuation which reduces the high frequency components and causing the low frequency gas shadow. The reservoir model for Ketzin contains several sandy permeable layers surrounded by clay and claystone. Therefore, a possible explanation for the low frequency gas shadow here may be related to the conversion of seismic P-waves from fast P-waves to slow P-waves and back to fast P-waves within the gas bearing layers. Permeable layers, partially saturated with gas, could increase the low frequency content of reflections with redistribution of energy from first phase to tail. These delays then results in low frequency shadows (Goloshubin and Silin 2006; Goloshubin personal communication 2007).

The Continuous Wavelet Transform method can be used as a quick indicator of gas (hydrocarbon) migration and will be an important technique in the monitoring phase of the CO_2SINK project.

Acknowledgment

We acknowledge the CO_2SINK consortium for providing the complementary data set and publication permission. We would like also to thank dGB Earth Sciences Company for providing the “Opendtect” software for this study. The European Commission is gratefully acknowledged for funding

CO2 Storage by Injection into a Natural Storage site CO2SINK, Project no. 502599.

We also acknowledge two anonymous reviewers for their constructive comments and suggestions.

The first author sincerely thanks the Iranian Offshore Oil Company and Central Training of the National Iranian Oil Company for funding his PhD studies at Uppsala University.

List of Figures

lines.

Figure 9. Similarity time slices for a) 215 ms (near top gas) and b) 160 ms. The fault system of the Ketzin structure is accurately mapped by the cube similarity attribute.

References

Castagna J. P., Sun S., and Siegfried R. 2003. Instantaneous spectral analysis: Detection of low-frequency shadows associated with hydrocarbons. *The Leading Edge* **22**, 127-129.

Castagna J. P., and Sun S. 2006. Comparison of spectral decomposition methods. *First Break* **24 (3)**. 75-79.

Ebrom D., 2004. The low frequency gas shadows in seismic sections. *The Leading Edge* **23**, 772.

Förster A., Norden B., Zinck-Jørgensen K., Frykman P., Kulenkampff J., Spangenberg E., Erzinger J., Zimmer M., Kopp J., Borm G., Juhlin C., Cosma C. and Hurter S. 2006. Baseline characterization of CO2SINK geological storage site at Ketzin, Germany. *Environmental Geosciences* **13**, 145-160.

Frykman P., Zinck-Jørgensen K., Bech N., Norden B., Förster A., and Larsen M. 2006. Site characterization of fluvial, incised-valley deposits. CO2SC symposium *Proceedings*, Lawrence Berkeley National laboratory, Berkeley, USA, 121-123.

Goloshubin G. M. and Bakulin A.V. 1998. Seismic reflectivity of a thin porous fluid saturated layer versus frequency. 68th SEG Meeting, New Orleans, USA, Expanded Abstracts, 976–979.

Goloshubin G. M., and Korneev V. A. 2000, Seismic low-frequency effects from fluid saturated reservoir. 70th SEG Meeting, Calgary, Canada, Expanded Abstracts, 1671-1674.

Goloshubin G. M., and Silin D. 2006, Frequency-dependent seismic reflection from a permeable boundary in a fractured reservoir. 76th SEG Meeting, New Orleans, USA, Expanded Abstracts, 1742-1746.

Goloshubin G. M., Korneev V. A., Silin D. B., Vingalov V. S. and VanSchuyer C. 2006. Reservoir imaging using low frequencies of seismic reflections. *The Leading Edge* **25,** 527-531.

Juhlin C., Giese R., Zinck-Jørgensen K., Cosma, C., Kazemeini H., Juhojuntti N., Luth S., Norden B., and Förster A. 2007. 3D baseline seismics at Ketzin, Germany: The CO2SINK project. *Geophysics* **72,** 121-132.

Korneev V. A., Goloshubin G.M., Daley T. M. and Silin D. B. 2004. Seismic low frequency effects in monitoring fluid-saturated reservoirs: *Geophysics* **69,** 522-532.

Partyka G. J., Gridley J., and Lopez J. 1999. Interpretational applications of spectral decomposition in reservoir characterization. *The Leading Edge* **18,** 353-360.

Scheck M., and Bayer U. 1999. Evolution of the Northeast German Basin Inferences from a 3D structural model and subsidence analysis. *Tectonophysics* **313,** 145-169.

Sinha S., Routh P. S., Anno P. D., and Castagna J. P. 2005. Spectral decomposition of seismic data with continuous-wavelet transforms. *Geophysics* **70,** 19-25.

Taner M. T., Koehler F. and Sherrif R. E. 1979. Complex seismic trace analysis. *Geophysics* **44,** 1041–1063.

Wang Y. 2003. Seismic time-frequency spectral decomposition by matching pursuit. *Geophysics* **72,** V13-V20.

Wurster P. 1964 Geologie des Schilfsandsteins. Mitteilungen des Geologischen Staatsinstitutes Hamburg **33**,140p.

Yordkayhun S., Ivanova A., Giese R., Juhlin C., Cosma C., 2007. Comparison of surface seismic sources at the CO2SINK site, Ketzin, Germany. Submitted to *Geophysical Prospecting*.

Ziegler P. A., 1990, *Geological atlas of western and central Europe*. Shell Internationale Petroleum Mij. B.V.

Table 1. Processing steps applied to the full 3D data set (Juhlin et al. 2007).

Step	Parameters
1	Read raw SEGD data
2	Extract and apply geometry
3	Trace edit and polarity reversal
4	Pick first breaks: offset range 300–500 m
5	Remove 50-Hz noise on selected receiver locations
6	Spherical divergence correction: v2t
7	Band-pass filter: Butterworth 7–14–150–250 Hz
8	Surface consistent deconvolution: filter 120 ms, gap 16 ms, white noise 0.1%
9	Ground roll mute
10	Spectral equalization 20–40–90–120 Hz
11	Band-pass filter: 0–300 ms: 15–30–85–125 Hz 350–570 ms: 14–28–80–120 Hz 620–1000 ms: 12–25–70–105 Hz
12	Zero-phase filter
13	Refraction statics: datum 30 m, replacement velocity 1800 m/s, v0 1000m/s
14	Trace balance using data window
15	Velocity analysis: every 20th CDP in the inline and crossline direction
16	Residual statics
17	Normal moveout correction: 50% stretch mute
18	Stack
19	Post-Stack processing
20	Migration: 3D FD using smoothed stacking velocities

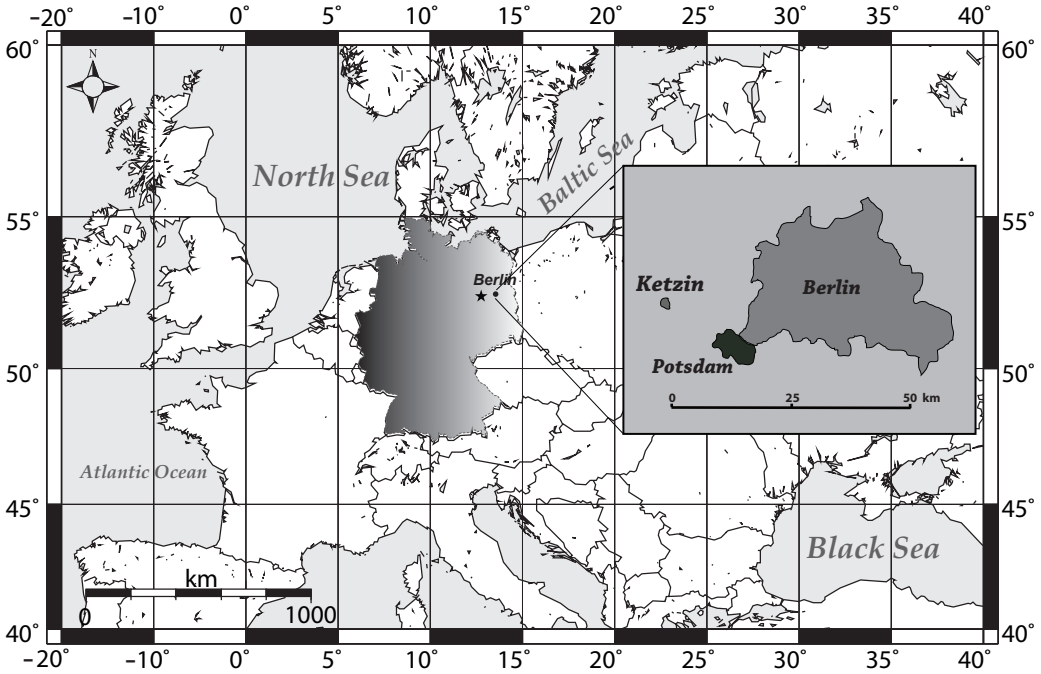
North Sea
Baltic Sea
Atlantic Ocean
Black Sea
Berlin
Ketzin
Berlin
Potsdam
0
25
50 km
km
0
1000
-20°
-10°
0°
5°
10°
15°
20°
25°
30°
35°
40°
60°
55°
50°
45°
40°
N

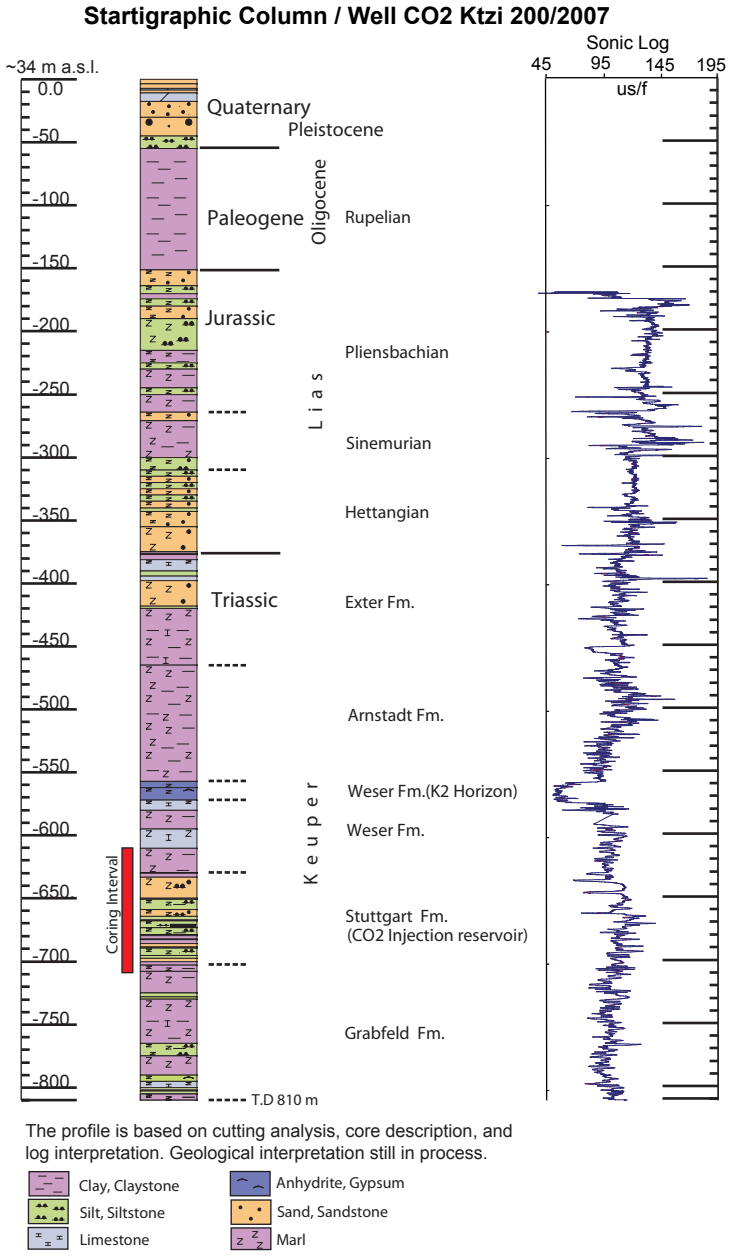
Startigraphic Column / Well CO2 Ktzi 200/2007
~34 m a.s.l.
0.0
-50
-100
-150
-200
-250
-300
-350
-400
-450
-500
-550
-600
-650
-700
-750
-800
Quaternary
Pleistocene
Paleogene
Oligocene
Rupelian
Jurassic
Pliensbachian
Liass
Sinemurian
Hettangian
Triassic
Exter Fm.
Arnstadt Fm.
Keuper
Weser Fm.(K2 Horizon)
Weser Fm.
Stuttgart Fm.
(CO2 Injection reservoir)
Grabfeld Fm.
T.D 810 m
Coring Interval
Sonic Log
45
95
145
195
us/f
The profile is based on cutting analysis, core description, and
log interpretation. Geological interpretation still in process.
Clay, Claystone
Silt, Siltstone
Limestone
Anhydrite, Gypsum
Sand, Sandstone
Marl

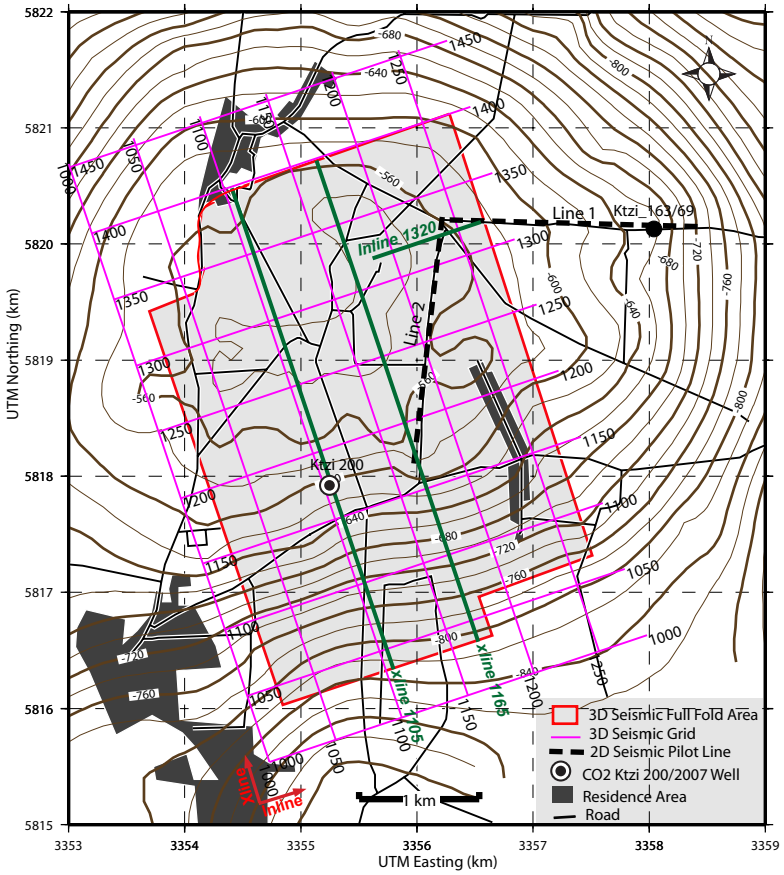
UTM Northing (km)
UTM Easting (km)
Line 1
Ktzi_163/69
Line 2
Ktzi 200
inline 1320
xline 1165
xline 1105
3D Seismic Full Fold Area
3D Seismic Grid
2D Seismic Pilot Line
CO2 Ktzi 200/2007 Well
Residence Area
Road
1 km

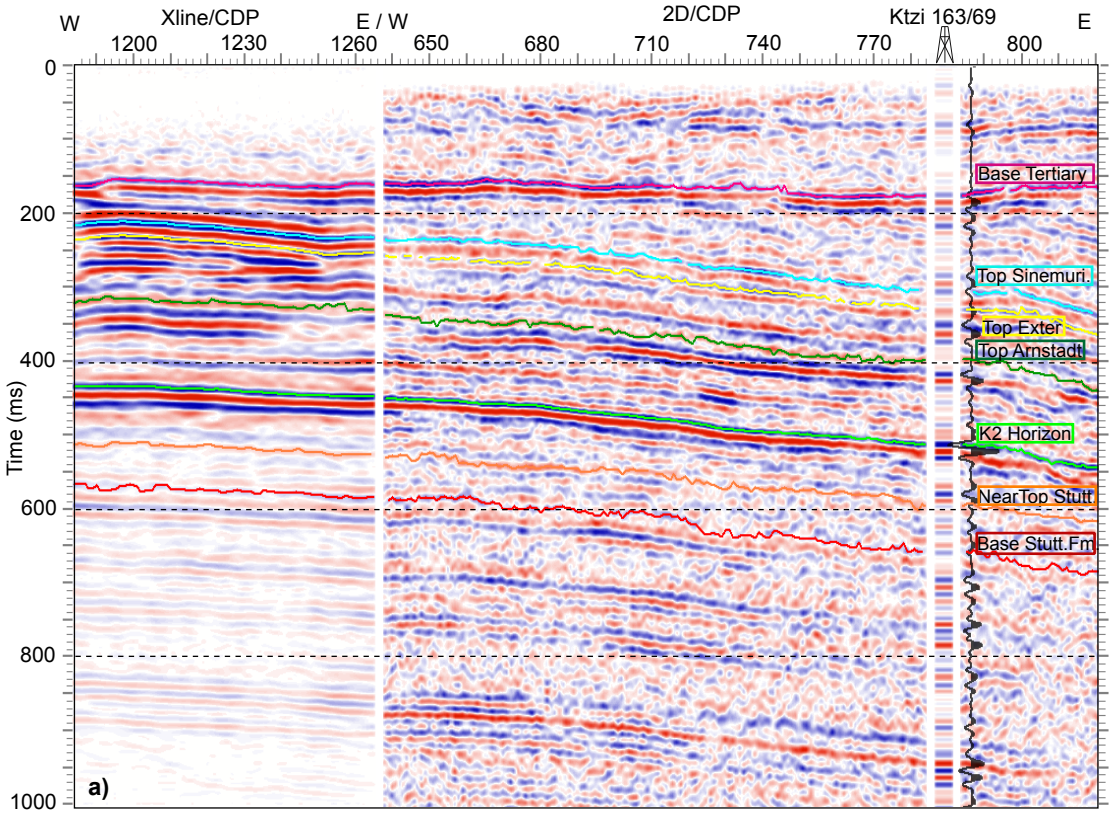
W
Xline/CDP
1200
1230
E / W
1260
650
2D/CDP
680
710
740
Ktzi 163/69
770
800
E
Time (ms)
0
200
400
600
800
1000
Base Tertiary
Top Sinemuri.
Top Exter
Top Arnstadt
K2 Horizon
NearTop Stutt
Base Stutt.Fm
a)

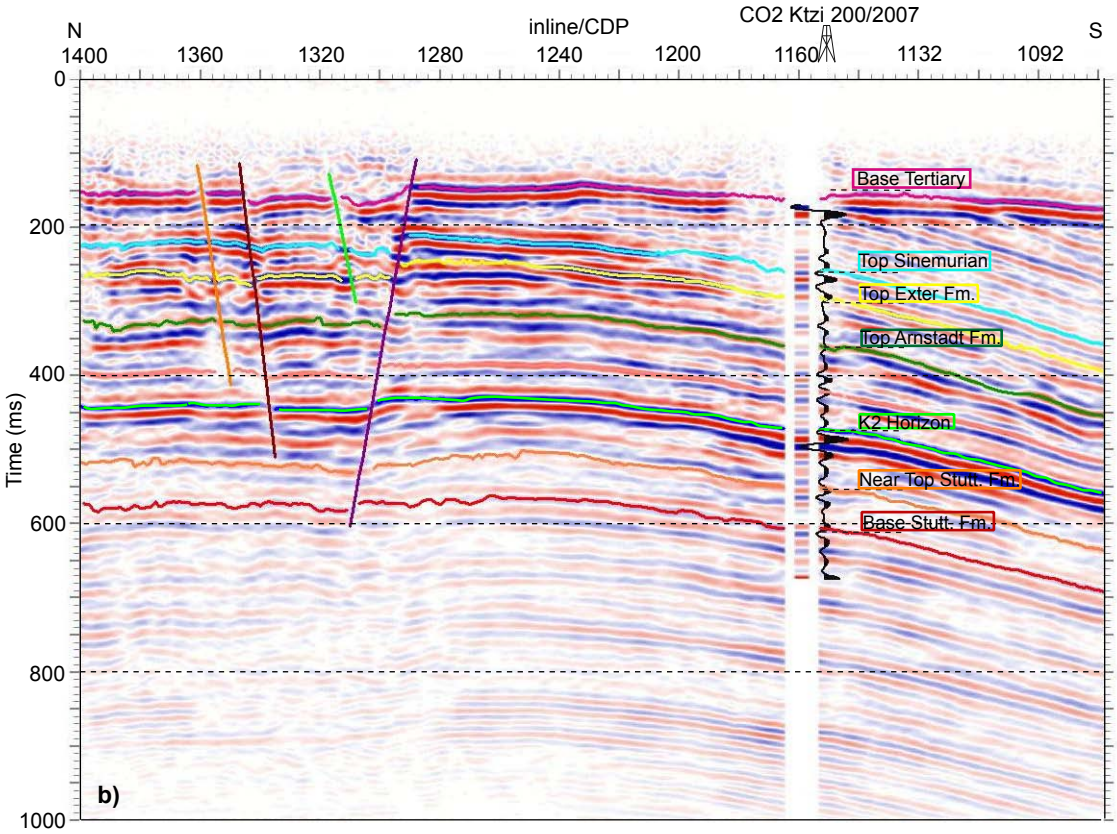
N
1400
1360
1320
1280
inline/CDP
1240
1200
CO2 Ktzi 200/2007
1160
1132
1092
S
Time (ms)
0
200
400
600
800
1000
Base Tertiary
Top Sinemurian
Top Exter Fm.
Top Arnstadt Fm.
K2 Horizon
Near Top Stutt. Fm.
Base Stutt. Fm.
b)

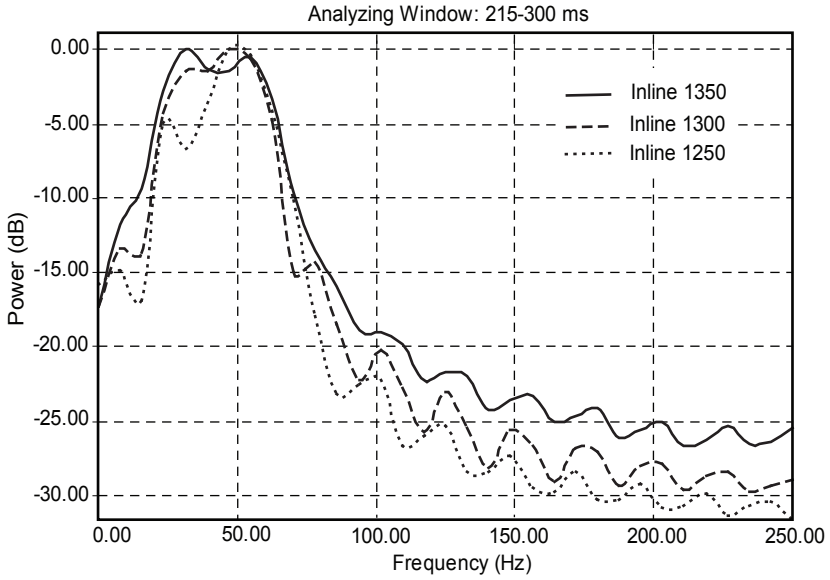
Power Spectra
Analyzing Window: 215-300 ms
Inline 1350
Inline 1300
Inline 1250
Power (dB)
0.00
-5.00
-10.00
-15.00
-20.00
-25.00
-30.00
0.00
50.00
100.00
150.00
200.00
250.00
Frequency (Hz)

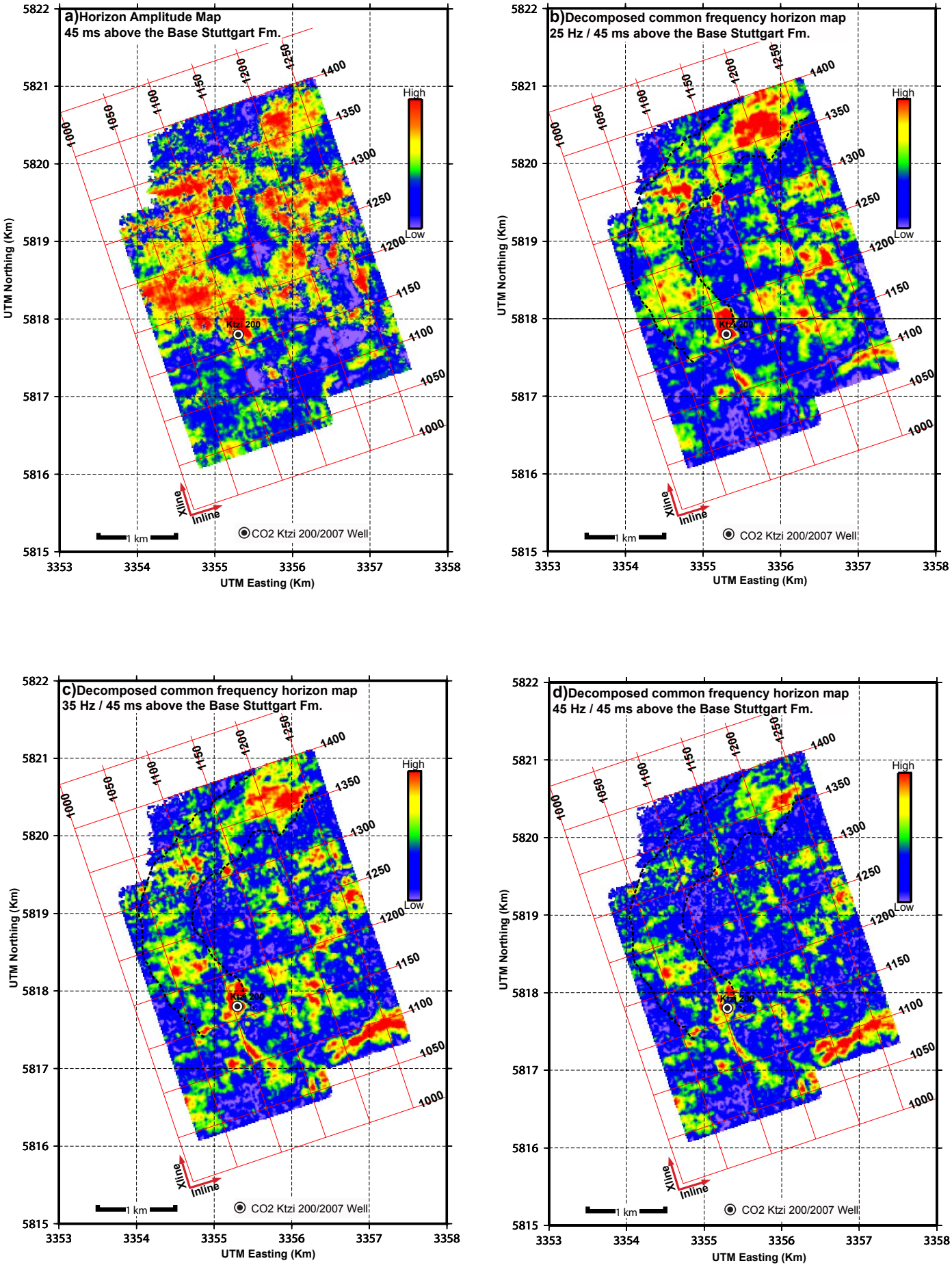
a)Horizon Amplitude Map
45 ms above the Base Stuttgart Fm.
b)Decomposed common frequency horizon map
25 Hz / 45 ms above the Base Stuttgart Fm.
c)Decomposed common frequency horizon map
35 Hz / 45 ms above the Base Stuttgart Fm.
d)Decomposed common frequency horizon map
45 Hz / 45 ms above the Base Stuttgart Fm.
High
Low
Ktzi 200
CO2 Ktzi 200/2007 Well
1 km
Xline
Inline
UTM Northing (Km)
UTM Easting (Km)
5822
5821
5820
5819
5818
5817
5816
5815
3353
3354
3355
3356
3357
3358
1000
1050
1100
1150
1200
1250
1300
1350
1400

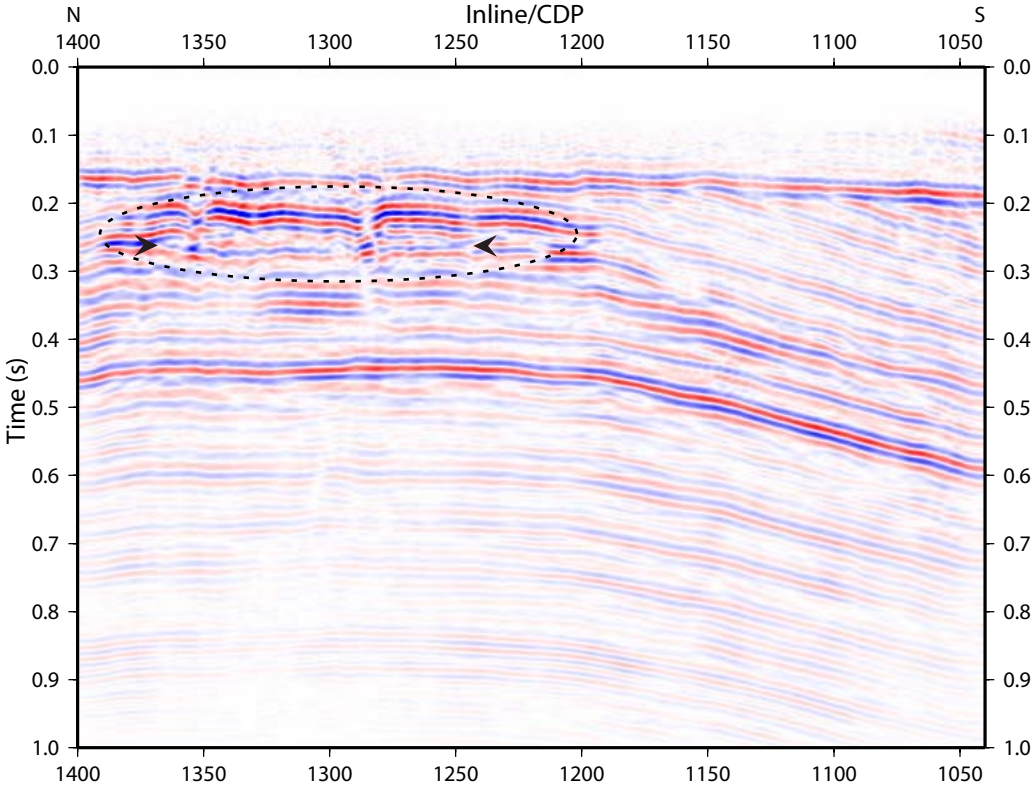
N
Inline/CDP
S
1400
1350
1300
1250
1200
1150
1100
1050
Time (s)
0.0
0.1
0.2
0.3
0.4
0.5
0.6
0.7
0.8
0.9
1.0

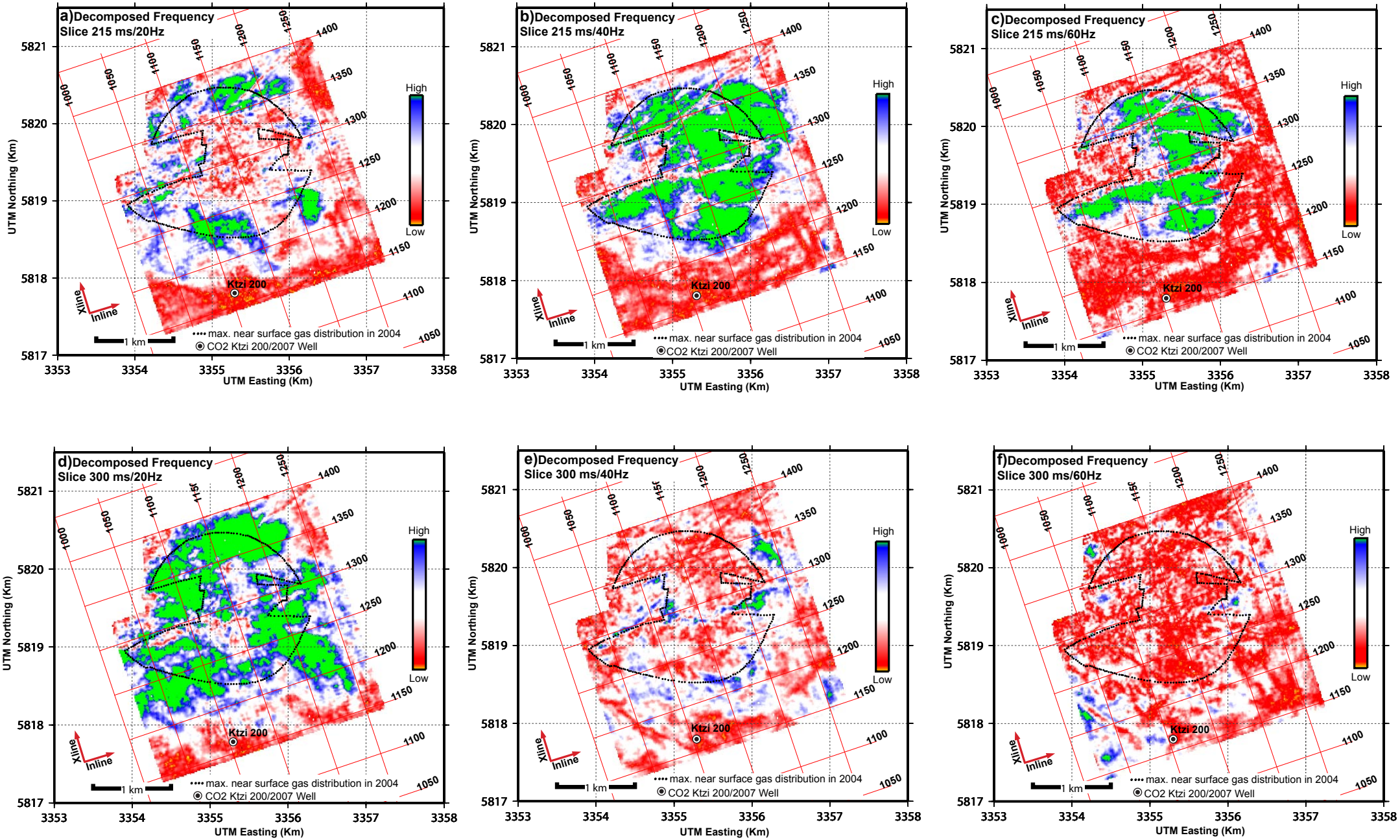
a)Decomposed Frequency
Slice 215 ms/20Hz
b)Decomposed Frequency
Slice 215 ms/40Hz
c)Decomposed Frequency
Slice 215 ms/60Hz
d)Decomposed Frequency
Slice 300 ms/20Hz
e)Decomposed Frequency
Slice 300 ms/40Hz
f)Decomposed Frequency
Slice 300 ms/60Hz
High
Low
Ktzi 200
Xline
Inline
1 km
max. near surface gas distribution in 2004
CO2 Ktzi 200/2007 Well
UTM Northing (Km)
UTM Easting (Km)
5817
5818
5819
5820
5821
3353
3354
3355
3356
3357
3358

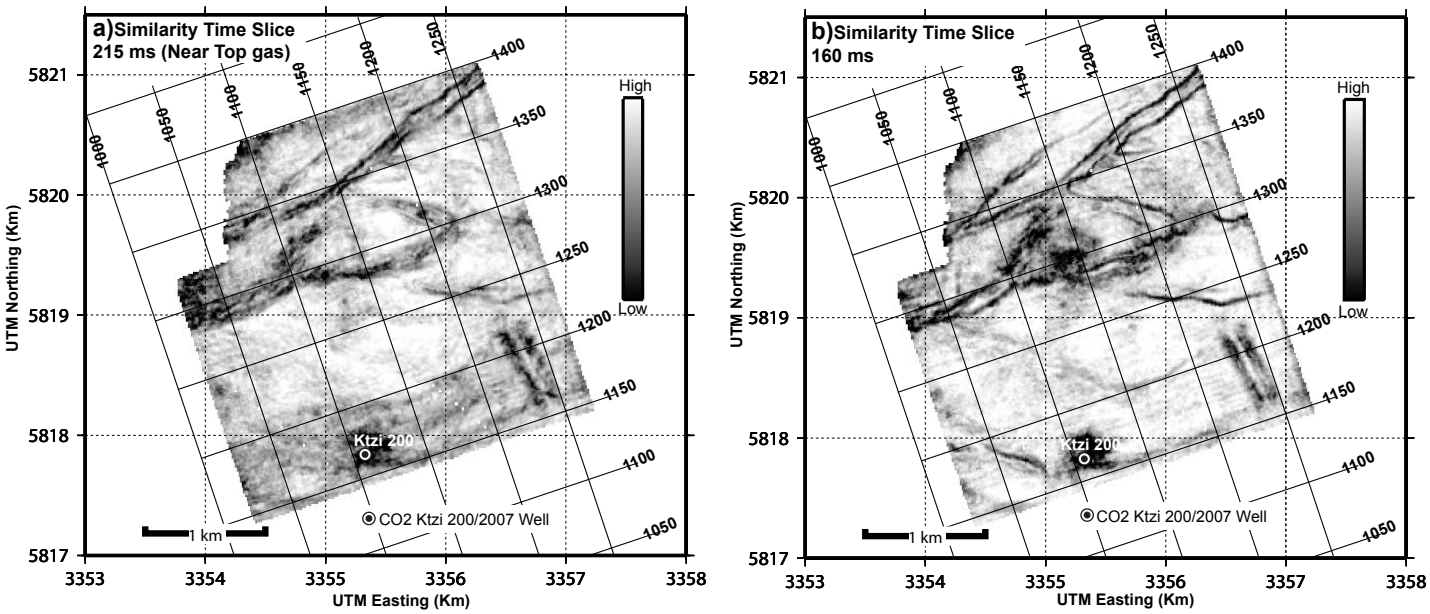
a)Similarity Time Slice
215 ms (Near Top gas)
b)Similarity Time Slice
160 ms
High
Low
Ktzi 200
CO2 Ktzi 200/2007 Well
1 km
UTM Northing (Km)
UTM Easting (Km)
5817
5818
5819
5820
5821
3353
3354
3355
3356
3357
3358